Superhydrophobic anti-ultraviolet films by doctor blade coating ⊘

Chang-Yun Cai; Kun-Yi Andrew Lin ; Hongta Yang

Check for updates

View Online   Export Citation   CrossMark

Articles You May Be Interested In

Macroporous photonic crystal-based vapor detectors created by doctor blade coating

Appl. Phys. Lett. (January 2011)

Macroporous photonic crystal-based anti-ultraviolet and anti-near-infrared materials by doctor blade coating

Appl. Phys. Lett. (February 2016)

Physics Doctorates

Physics Today (March 1964)

AIP Publishing

Superhydrophobic anti-ultraviolet films by doctor blade coating

Chang-Yun Cai,[1] Kun-Yi Andrew Lin,[2] and Hongta Yang[1,a]

[1]*Department of Chemical Engineering, National Chung Hsing University, 250 Kuo Kung Road, Taichung 40227, Taiwan*
[2]*Department of Environmental Engineering, National Chung Hsing University, 250 Kuo Kung Road, Taichung 40227, Taiwan*

This article reports a scalable technology for fabricating polymer films with excellent water-repelling and anti-ultraviolet properties. A roll-to-roll compatible doctor blade coating technology is utilized to prepare silica colloidal crystal-polymer composites. The silica microspheres can then be selectively removed to create flexible self-standing macroporous polymer films with crystalline arrays of pores. The void sizes are controlled by tuning the duration of a reactive ion etching process prior to the removal of the templating silica microspheres. After surface modification, superhydrophobic surface can be achieved. This study further demonstrates that the as-prepared transparent porous films with 200 nm of pores exhibit diffraction of ultraviolet lights originated from the Bragg's diffractive of light from the three-dimensional highly ordered air cavities. © 2014 AIP Publishing LLC.
[http://dx.doi.org/10.1063/1.4902547]

Through years of evolution, biological systems have developed a wide spectrum of unique architectures for advanced functionalities.[1–3] Inspired by the lotus effect, superhydrophobic coatings have been developed to provide superior water repellency and protections for almost any surface. It is well-known that the combination of low surface energy materials with hierarchical structures, that is the origin of lotus leaves, is an efficient approach to fabricate superhydrophobic coatings.[4–6] As air is the most common hydrophobic material, porous coatings with a large fraction of entrapped air have been extensively exploited to control the wettability of the films. A large variety of methodologies have been demonstrated to create water-repellent coatings on various substrates.[7–11]

Self-assembly of colloidal particles is an inexpensive and simple technology for creating highly ordered colloidal crystals, which can be used as templates to produce superhydrophobic macroporous films.[12–14] The prepared macroporous films, which are with crystalline arrays of pores, are intrinsic three-dimensional photonic crystals, exhibiting unique optical diffraction caused by Bragg diffraction.[15,16] Photonic crystals based on macroporous films have been arousing wide research interests due to their structure color with respect to pore size. With a growing interest, numbers of studies have been recently reported on the preparation of ultraviolet-shielding materials via introduction of photonic crystals.[17–21] However, many of current approaches are favorable only for low-volume, laboratory-scale production. Furthermore, to the extent of our knowledge, transparent macroporous films with water-repellent and ultraviolet-shielding properties are not available.

In this study, macroporous polymer photonic crystals with three-dimensional highly ordered crystalline arrays of pores are fabricated by a simple and roll-to-roll compatible doctor blade coating technology.[22,23] The fabrication process for creating superhydrophobic macroporous polymer films is shown in Figure 1. The 200 nm silica particles are dispersed in ethoxylated trimethylolpropane triacrylate (ETPTA) monomer to make colloidal suspension with a particle volume fraction of 75%. The suspension is doctor blade coated at 1 mm/min on a glass which has been coated by an ETPTA wetting layer. The monomer is photo-polymerized to form a colloidal crystal-polymer composite. The polymer matrix is then etched by using a reactive ion etcher operating at 40 mTorr oxygen pressure, a 40 sccm flow rate, and 100 W to partially release the embedded top-layer silica microspheres for various durations. The embedded silica microspheres can be etched by a 2 vol. % hydrofluoric acid aqueous solution. The resulting macroporous polymer film is finally surface-modified by (tridecafluoro-1,1,2,2-tetrahydrooctyl) trichlorosilane in an oven at 120 °C to decrease surface energy.[24]

Figures 2(a) and 2(b) show a photograph and a cross-sectional scanning electron microscope (SEM) image of a doctor blade coated silica colloidal crystal-ETPTA composite, respectively. The composite exhibits uniform shining blue color caused by Bragg diffraction of blue light from long-range hexagonal ordering of silica colloidal crystals. The embedded silica microspheres can be wet-etched, leading to a self-standing transparent macroporous film [Figure 2(c)]. The crystalline ordering of hexagonal close-packed air cavities is clearly found in Figure 2(d). This indicates that the macroporous polymer films with three-dimensional crystalline arrays of pores are fabricated by the scalable doctor blade coating technology.

Top-view SEM images of plasma etched macroporous polymer films are shown in Figure 3. Figure 3(a) shows the polymer films exhibiting long-range hexagonal ordering of pores. The films are fabricated by oxygen plasma which etches the doctor blade coated colloidal crystal-polymer composite for various durations, followed by removal of the templating 200 nm silica microspheres. The top-layer void sizes are measured by averaging 100 cavities, and summarized in Figure 4(a). The results disclose that the void size increases with plasma etching time at the beginning, and
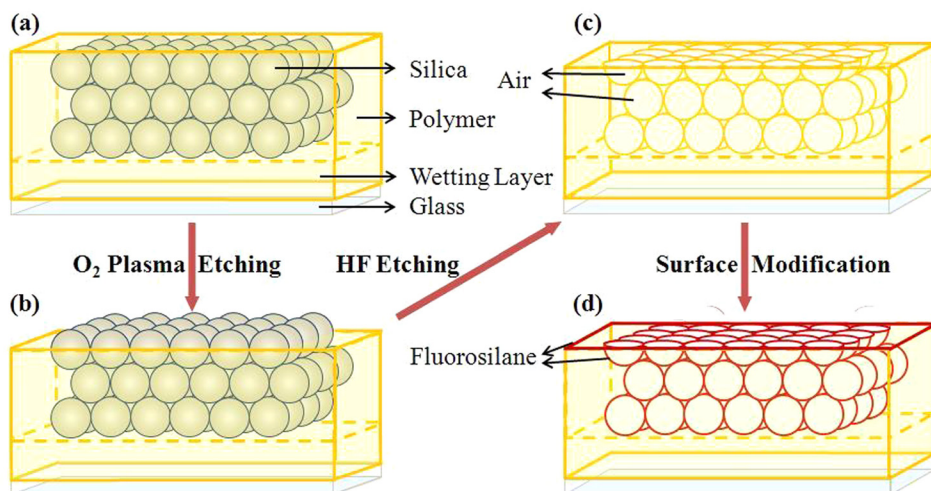
a)E-mail: hyang@dragon.nchu.edu.tw

   105, 201913-1

FIG. 1. Schematic illustration of the fabrication process for creating super-hydrophobic macroporous polymer films.

smaller void size is obtained as only bottom parts of the silica microspheres are templated after plasma etching for 60 s. The top-layer air cavities sketches with various etching time are shown in the insets of Figures 3(b)–3(h), respectively. It is also found that top-hemisphere of top-layer silica microspheres are revealed after the plasma etching for 50 s, leading to a maximal void size (196 ± 3 nm), which is close to the diameter of templating silica microspheres.

The hydrophobicity of the plasma etched macroporous film is improved by functionalizing with fluorosilane. The static water contact angles (SWCA) of the surface modified films are measured by a sessile drop shape analysis system (KRÜSS G10), and the results are disclosed in Figure 4(b) by averaging ten measurements on each sample. It is apparent that the SWCAs follow similar tendency as the void sizes under different etching durations. The SWCA increases until a maximal contact angle of 152° ± 4° [inset of Figure 4(b)] is reached at a plasma etching time of 55 s. For longer plasma

etching time, the formation of smaller void size on macroporous film reduces the SWCA. The above experimental results indicate that superhydrophobic coatings with SWCA larger than 150° can be achieved. The observations can furthermore be explained by adopting Cassie's equation

$$\cos \theta' = f \cos \theta - (1 - f), \tag{1}$$

where θ' is the static water contact angle on a rough surface, θ is the intrinsic water contact angle on a flat surface, and f is the fraction of the area of the polymer in direct contact with the water droplet. Figure 4(a) shows estimated f by applying the following trigonometric calculation:

$$f = 1 - \left(\frac{\pi R_v^2}{2\sqrt{3} R_s^2} \right), \tag{2}$$

where R_v is the radius of voids measured by the SEM images shown in Figure 3, and R_s is the radius of the templating
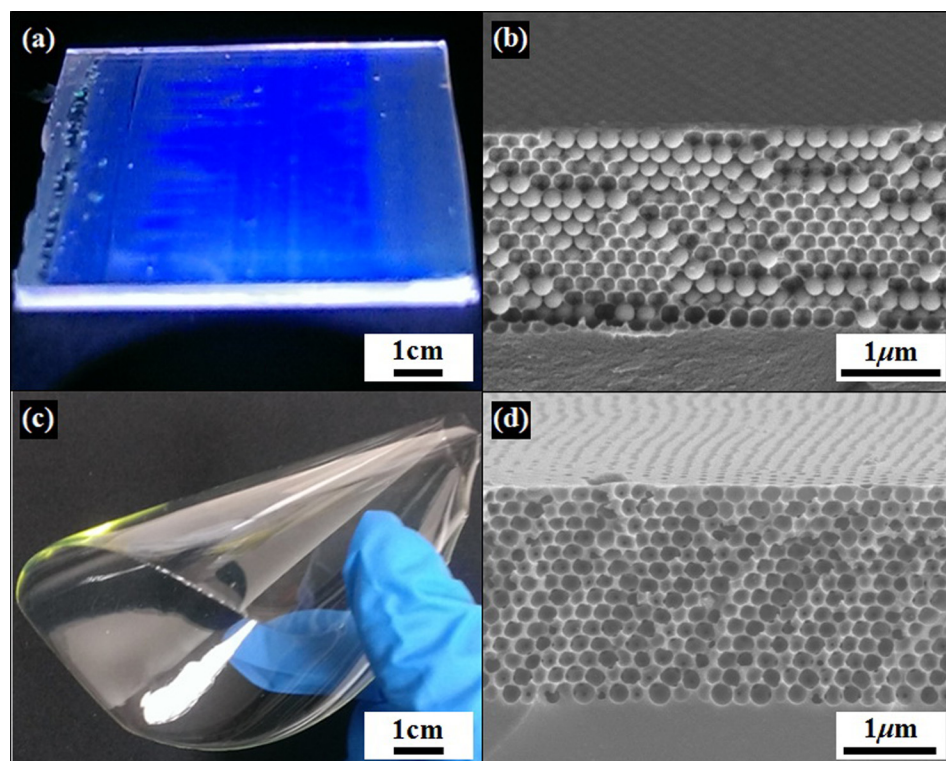
FIG. 2. (a) Photography of a doctor blade coated silica colloidal crystal-ETPTA composite consisting of 200 nm silica microspheres. (b) Cross-sectional SEM image of the same sample as in (a). (c) Photography of a self-standing macroporous ETPTA film template from 200 nm silica microspheres. (d) Cross-sectional SEM image of the same sample as in (c).
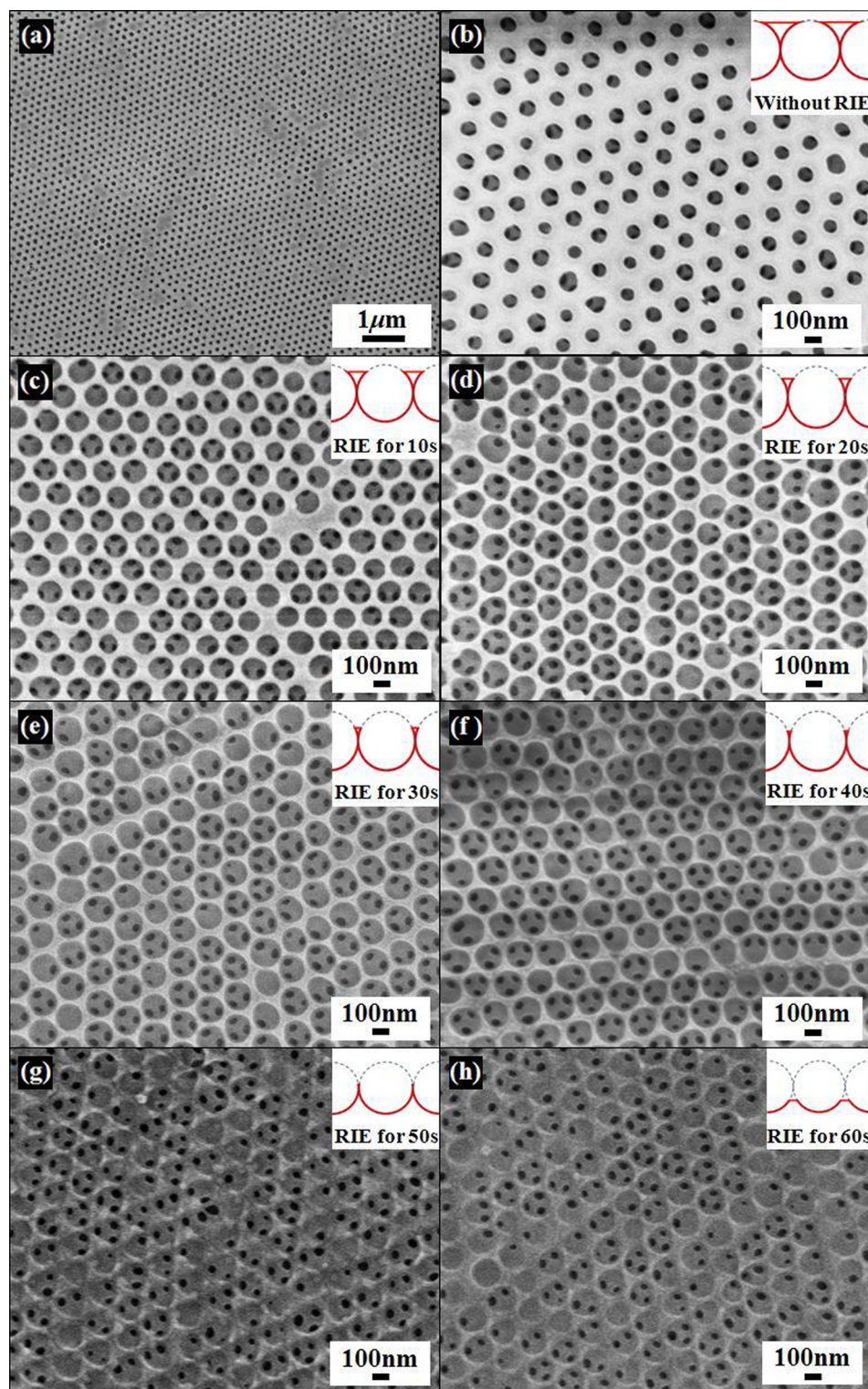
FIG. 3. (a) Top-view SEM images of macroporous ETPTA film template from 200 nm silica microspheres. (b) Magnified image of (a). Top-view SEM images of macroporous ETPTA films fabricated by oxygen plasma etching a composite for (c) 10, (d) 20, (e) 30, (f) 40, (g) 50, and (h) 60 s, followed by selective removal of the templating silica microspheres.

200 nm silica microspheres. It is clear that f value follows the same trend as the void size. The calculated water contact angles using Cassie's equation are compared with the experimental data in Figure 4(b). The tendencies of experimental and calculated results are similar, indicating that the Cassie's model is valid for the as-prepared superhydrophobic macroporous polymer films.

To evaluate the optical properties of doctor blade coated silica colloidal crystal-polymer composite and macroporous polymer film, Ocean Optics UV-Vis-NIR spectrometer is applied to measure the optical reflection and transmission at normal incidence. Figure 5(a) displays the diffraction peak of the composite consisting of 200 nm silica microspheres and an ETPTA matrix locates at 460 nm. The low refractive index contrast of silica colloidal crystal-polymer composite results in the low reflection amplitude of the corresponding spectra. Figure 5(a) also indicates that the diffraction peak of the corresponding macroporous ETPTA film locates at 361 nm with a high reflection amplitude. It reveals that the as-prepared macroporous film can reflect around 90% of incident ultraviolet radiation, resulted from the high refractive index contrast of air cavities and polymer matrix.
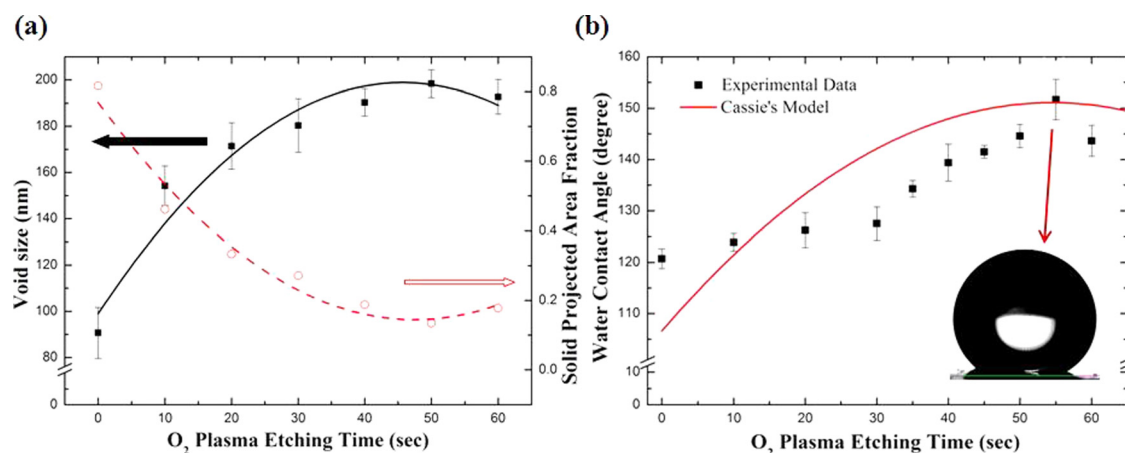
FIG. 4. (a) Dependence of the void size and the corresponding projected area fraction of macroporous ETPTA films template from 200 nm silica microspheres at different oxygen plasma etching durations. (b) Experimental and calculated static water contact angles of the surface modified macroporous films etched at different oxygen plasma etching durations.
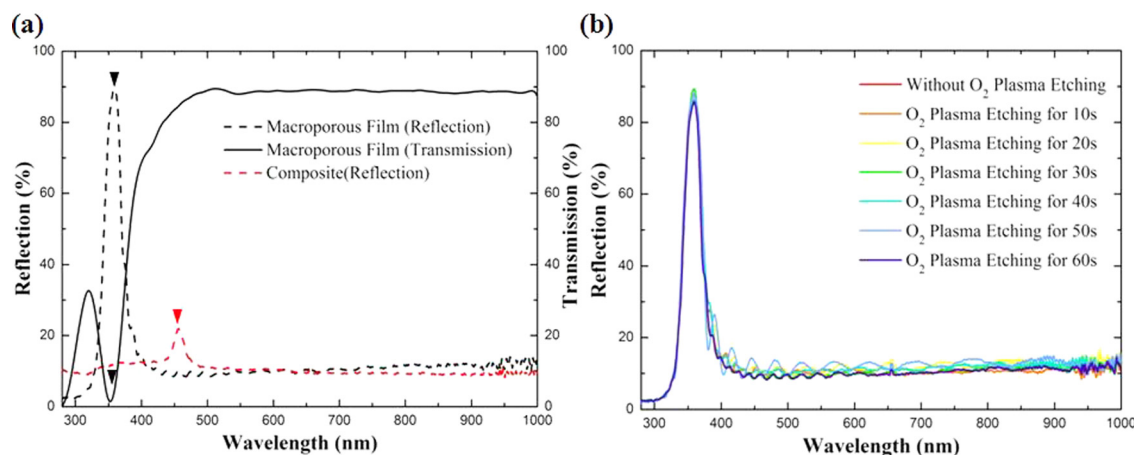

FIG. 5. (a) Normal incidence optical spectra of a silica colloidal crystal-ETPTA composite consisting of 200 nm silica microspheres, and a corresponding macroporous ETPTA film. The arrows indicate the expected positions of the peaks for each sample, calculated using Bragg's law at normal incidence. (b) Normal incidence optical reflection spectra obtained from macroporous ETPTA films fabricated by oxygen plasma etching a composite at different durations.

Besides that the normal incidence transmission spectrum shown in Figure 5(a) discloses that the average ultraviolet light and visible light transmittance of the macroporous polymer film are around 3% and 90%, respectively. This further demonstrates the transparency of the macroporous film revealed in Figure 2(c). The positions of the diffraction peaks can be theoretically calculated by using Bragg's law[25]

$$\lambda_{peak} = 2n_{eff}d\sin\theta, \qquad (3)$$

where n_{eff} is the effective refractive index of the medium, d is the interlayer spacing, and $\sin\theta = 1$ at normal incidence. The calculated peak positions as shown by the indicating arrows agree with experimental results, confirming that the self-assembled macroporous films are with high crystalline quality of pores. Besides that the normal-incidence specular reflection spectra obtained from macroporous films with different oxygen plasma etching durations are shown in Figure 5(b). The optical reflectance measurements on seven samples display that the shift of peak position is less than 1 nm for all the samples, disclosing that the anti-ultraviolet capability does not affect by top-layer void size during plasma etching process. The slight reduction of the reflection amplitude of

the corresponding spectra is caused by the partially collapsed structure of the macroporous films during the plasma etching process shown in Figure 3.

In summary, this research has demonstrated that transparent anti-ultraviolet macroporous polymer films can be fabricated by a scalable and roll-to-roll compatible doctor blade coating technology. The resulting macroporous films exhibit superhydrophobic surface with high static water contact angle after oxygen plasma etching and surface functionalization procedures.

[1]C.-H. Sun, B. Jiang, and P. Jiang, Appl. Phys. Lett. **92**, 061112 (2008).
[2]Y. M. Zheng, H. Bai, Z. B. Huang, X. L. Tian, F. Q. Nie, Y. Zhao, J. Zhai, and L. Jiang, Nature **463**, 640 (2010).
[3]H. Yang and P. Jiang, Appl. Phys. Lett. **98**, 011104 (2011).
[4]T. Darmanin, E. T. de Givenchy, S. Amigoni, and F. Guittard, Adv. Mater. **25**, 1378 (2013).
[5]K. S. Liu, Y. Tian, and L. Jiang, Prog. Mater. Sci. **58**, 503 (2013).
[6]J. V. I. Timonen, M. Latikka, L. Leibler, R. H. A. Ras, and O. Ikkala, Science **341**, 253 (2013).

[7]S. G. Park, H. H. Moon, S. K. Lee, J. Shim, and S. M. Yang, Langmuir **26**, 1468 (2010).

[8]N. Q. Zhan, Y. X. Li, C. Q. Zhang, Y. Song, H. G. Wang, L. Sun, Q. B. Yang, and X. Y. Hong, J. Colloid Interface Sci. **345**, 491 (2010).

[9]Y. Lai, F. Pan, C. Xu, H. Fuchs, and L. Chi, Adv. Mater. **25**, 1682 (2013).

[10]Y. Huang, J. M. Zhou, B. Su, L. Shi, J. X. Wang, S. R. Chan, L. B. Wang, J. Zi, Y. L. Song, and L. Jiang, J. Am. Chem. Soc. **134**, 17053 (2012).

[11]H. Yang, X. Dou, Y. Fang, and P. Jiang, J. Colloid Interface Sci. **405**, 51 (2013).

[12]E. J. Lee, J. J. Kim, and S. O. Chio, Langmuir **26**, 3024 (2010).

[13]O. Sato, S. Kubo, and Z. Z. Gu, Acc. Chem. Res. **42**, 1 (2009).

[14]S. H. Kim, S. Y. Lee, and S. M. Yang, Angew. Chem. Int. Ed. **49**, 2535 (2010).

[15]P. Jiang, J. Cizeron, J. F. Bertone, and V. L. Colvin, J. Am. Chem. Soc. **121**, 7957 (1999).

[16]R. Rengarajan, P. Jiang, V. L. Colvin, and D. M. Mittleman, Appl. Phys. Lett. **77**, 3517 (2000).

[17]J. F. de Lima, R. F. Martins, C. R. Neri, and O. A. Serra, Appl. Surf. Sci. **255**, 9006 (2009).

[18]M. Aklaloucha, A. Callejaa, X. Granadosa, S. Ricarta, V. Boffab, F. Riccib, T. Puiga, and X. Obradors, Sol. Energy Mater. Sol. Cells **120**, 175 (2014).

[19]Y. Zhang, S. Zhuang, X. Xu, and J. Hu, Opt. Mater. **36**, 169 (2013).

[20]C.-H. Xue, W. Yin, P. Zhang, J. Zhang, P.-T. Ji, and S.-T. Ji, Colloids Surf. A **427**, 7 (2013).

[21]S. Li, M. S. Toprak, Y. S. Jo, J. Dobson, D. K. Kim, and M. Muhammed, Adv. Mater. **19**, 4347 (2007).

[22]H. Yang and P. Jiang, Langmuir **26**, 13173 (2010).

[23]H. Yang and P. Jiang, Langmuir **26**, 12598 (2010).

[24]F. A. Houle, C. T. Rettner, D. Miller, and R. Sooriyakumaran, Appl. Phys. Lett. **90**, 213103 (2007).

[25]P. Jiang, J. F. Bertone, K. S. Hwang, and V. L. Colvin, Chem. Mater. **11**, 2132 (1999).